Inorganic Chemistry

Article

pubs.acs.org/IC

m-Phthalic Diamide-Linked Zinc Bisporphyrinate: Spontaneous Resolution of Its Crystals and Its Application in Chiral Recognition of Amino Acid Esters

Jiaxun Jiang,[†,∥] Xianshi Fang,[†,∥] Baozhen Liu,[†] and Chuanjiang Hu*[,†,‡]

[†]Key Laboratory of Organic Synthesis of Jiangsu Province, College of Chemistry, Chemical Engineering and Materials Science, Soochow University, Suzhou 215123, P. R. China

[‡]State Key Laboratory & Coordination Chemistry Institute, Nanjing University, Nanjing 210093, P. R. China

Supporting Information

ABSTRACT: A novel *m*-phthalic diamide-linked zinc bisporphyrinate [Zn_2-**1**] has been designed and synthesized. Its chiral crystalline samples have been spontaneously resolved by crystallization. Data for $C_{48}H_{29}N_5OZn$ follow: tetragonal, $I4_1$, a = 17.809(2) Å, b = 17.809(2) Å, c = 27.080(8) Å, V = 8589 (3) Å^3, Z = 8. X-ray crystallography reveals the two porphyrin subunits are clockwise arranged in the solved structure. Each zinc atom is coordinated by four pyrrole nitrogens and the amide oxygen of the neighboring molecule. Through coordination bonds, it forms a helical chain with *P* configuration along the *c* axis. The overall crystal forms an unprecedented chiral bisporphyin coordination polymer. The chirality of the single crystals has been confirmed by CD spectroscopy. UV−vis and NMR spectroscopic studies suggested the molecule aggregates in solution. Such *m*-phthalic diamide-linked zinc bisporphyrinate shows a strong chiral recognition ability for amino acid ethyl esters. The amplitude value of the induced circular dichroism (ICD) (~1900 cm^{-1} M^{-1}) is around 10 times larger than the one observed for the oxalic amide-linked species (*Dalton Trans.* **2013**, *42*, 7651−7659). Further studies by ^{1}H NMR and UV−vis spectroscopies have revealed amino acid esters function as monodentate ligands, and [Zn_2-**1**] interacts with amino acid ethyl esters through coordination and hydrogen bonding interactions. The CD amplitude values have also shown dependence on the bulkiness of the side chain of amino acid esters. A possible chiral recognition mechanism has been proposed.

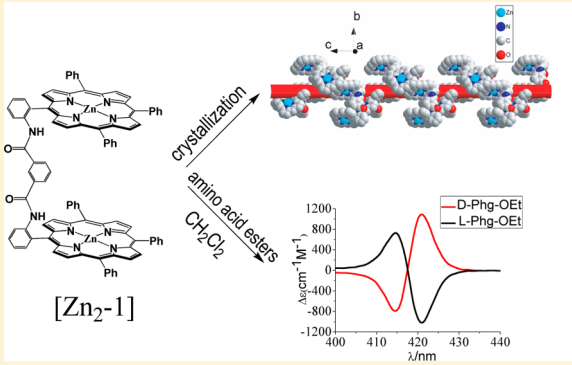

INTRODUCTION

Bisporphyrins have been intensively studied as chirality probes, sensors, etc. in recent years.[1] Many different bisporphyrin systems have been developed for various chiral guests. In most cases, their guest molecules function as bidentate ligands through complexation. For example, Berova, Nakanishi, and coworkers have designed a bisporphyrin unit linked by a pentanediol linker which was used to assign the absolute configuration of several chiral acyclic diamines, amino alcohols, and conjugates of primary amines, secondary amines, secondary alcohols, and α-chiral carboxylic acids by the intense bisignate CD signals in the Soret band region.[2] Borhan's group has developed a fluorinated porphyrin tweezer which can be used to determine the absolute configuration of diols, amino alcohols, diamines, and epoxy alcohols.[3] It is more difficult to find examples, in the literature, of guest molecules as monodentate ligands. One of these examples is the ethane-bridged bisporphyrin developed by Borovkov, Inoue, and coworkers, which can chirally recognize monoamine, monoalcohol, or amino acid esters.[4] In that system, the steric interactions have significant influence on the supramolecular chirality induction.

We have been working on porphyrin-related hydrogen bonds and chirality for several years.[5] We have recently developed an oxalic amide-linked zinc bisporphyrinate, which allows the chiral recognition of amino acid ethyl esters.[5e] The study suggests the following: (1) amino acid esters function as monodentate ligands in the chiral recognition process; (2) the rigid oxalic amide linkage makes the bisporphyrin adopt an *anti*-configuration; (3) one important hydrogen bond is formed between the coordinated nitrogen of amino acid esters and the carbonyl oxygen of the amide group. This study allowed us to directly determine the chirality for monodentate chiral guests.

In the case of the oxalic amide-linked zinc bisporphyrinate system, the total CD amplitude (A_{obs}, the sum of the maximum intensities of each Cotton effect in the couplet) is not quite large, only up to around 200 cm^{-1} M^{-1}. As we know from the exciton chirality theory method,[6] the total CD amplitude value of the exciton split CD is related to the dihedral angle between the projections of the two transition moments of the chromophores. This has been confirmed by several inves-

Received: July 27, 2013
Published: March 11, 2014

tigations. For example, the *A* value as shown in the case of simple dibenzoates has a parabolic dependence on the dihedral angle between the projections of the coupling transitions, with zero values at 0° and 180° and a maximum value at 70°.[7] Osuka and co-workers' studies on a series of rigidly *meso*−*meso*-linked bisporphyrins suggest the magnitude of the Cotton effects is dependent upon the angle between the transition dipole moments (which is also the angle between porphyrin planes in that case).[8] In that system, the *A* values reach a maximum at around 70° for the interelectronic transition angle.

For the case of the oxalic amide-linked species, the linkage is probably too rigid, and the corresponding angle between the projections of the electric transition moments (along the 5,15-axes of the porphyrin subunits) is around 156° (from DFT calculations).[5e] In order to further improve such amide-linked systems, we are trying to tune the flexibility of the bisporphyrin system by introduction of various substituents in the bridge between the two porphyrin subunits. If the linkage is less rigid, it may allow better interelectronic transition angles, and then it could lead to larger amplitude of ICD, and provide a better CD probe for chirality. With this in mind, we have chosen a more flexible group, *m*-phthalic diamide, as the linkage.

Herein, we have synthesized *m*-phthalic diamide-linked bisporphyrins, [Zn_2-**1**], as shown in Figure 1. For comparison,

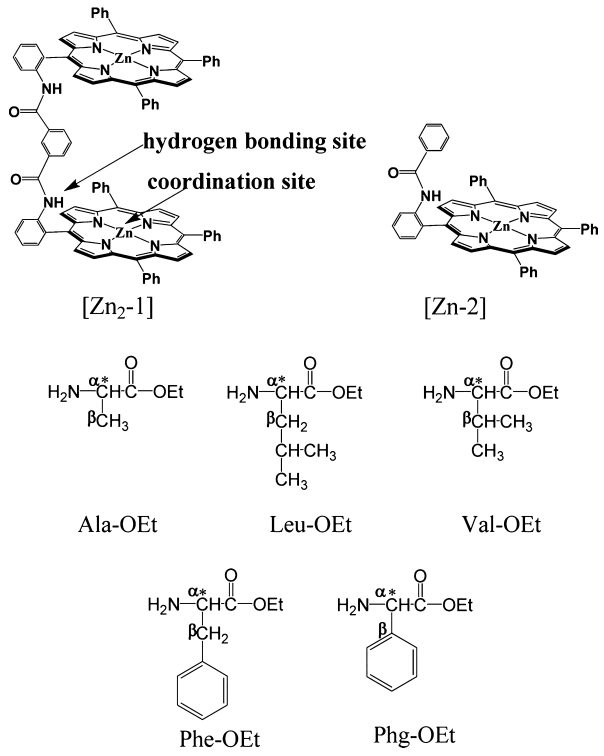

Figure 1. Structure formulas of the designed *m*-phthalic diamide-linked zinc bisporphyrinate ([Zn2-**1**]), zinc monoporphyrinate ([Zn-**2**]), and five amino acid ethyl esters.

monoporphyrin ([Zn-**2**]) has also been synthesized. Interestingly, crystals of [Zn_2-**1**] were spontaneously resolved upon crystallization. In the solved structure, [Zn_2-**1**] forms a helical chain with *P* configuration, and the overall crystal forms a coordination polymer. To the best of our knowledge, it is the first chiral bisporphyrin coordination polymer. More importantly, [Zn_2-**1**] has also shown a chiral recognition ability for amino acid esters. CD studies show the amplitude values are up to 1900 cm^{-1} M^{-1}. Its chiral recognition mechanism has also been discussed.

EXPERIMENTAL SECTION

Material and Physical Methods. All reagents were obtained from commercial sources without further purification unless otherwise noted. Pyrrole was freshly distilled before use. Triethylamine (Et_3N) was distilled over potassium hydroxide, and the methylene dichloride was treated with CaH_2 before use. All amino acid ethyl ester hydrochlorides used were purchased from commercial sources. The fresh distilled amino acid esters were prepared by reported methods.[9] The zinc 5-(2-aminophenyl)-10,15,20-triphenyl-porphyrinate was synthesized according to reported methods.[10]

Elemental analyses (C, H, and N) were performed with an Elementar Vario EL III analytical instrument. ^{1}H NMR spectra were carried out using a Bruker AVANCE 400 spectrometer or Bruker AVANCE III HD 400 MHz spectrometer equipped with a 5 mm PABBO BB-probe head in $CDCl_3$; chemical shifts are expressed in ppm relative to chloroform (7.26 ppm). UV−vis spectra were measured with a Shimadzu UV-3150 spectrometer. UV−vis spectra of [Zn_2-**1**] have been measured in 0.1 mm, 1 mm, and 1.0 cm quartz cell for different concentration as 1.63×10^{-7} M, 8.13×10^{-7} M, 1.63×10^{-6} M, 1.63×10^{-5} M, 1.63×10^{-4} M in CH_2Cl_2. CD spectra were recorded on an AVIV model 410 spectropolarimeter at 25 °C. Scanning conditions were as follows: wavelength step = 1.00 nm, bandwidth = 2 nm, response time = 0.1 s, averaging time = 0.100 s, settling time = 0.333 s.

General Procedure for CD Measurement. The background spectrum was taken from 380 to 460 nm with a scan rate of 100 nm/min at 25 °C. Zinc bisporphyrinate solution (2.40×10^{-6} M, 2.50 mL) was injected into a 1.0 cm quartz cuvette. Then, 4000 equiv of D-(or L-) amino acid esters were added into the above solution to form the corresponding complexes. CD spectra were measured after several minutes (minimum of 4 accumulations). The resultant ECCD spectra recorded in millidegrees were normalized on the basis of the zinc bisporphyrinate concentration.

^{1}H NMR and UV−Vis Titrations. For ^{1}H NMR titration experiments, the portions of a solution of D-leucine ethyl ester in $CDCl_3$ were added to the solution of [Zn_2-**1**] in $CDCl_3$ in a 5 mm o.d. NMR tube, and ^{1}H NMR spectra were taken after each addition. UV−vis titration experiments were carried out as follows. Portions of a solution of the D- (or L-) amino acid ethyl esters in CH_2Cl_2 were added to the solution of [Zn_2-**1**] in CH_2Cl_2 in a 1.0 cm quartz cell, and UV−vis spectra were taken after each addition.

Preparation of Free Base Bisporphyrin 1. The reaction was carried out under anaerobic conditions. 5-(2-Aminophenyl)-10,15,20-triphenylporphyrinate (0.57 g, 0.91 mmol) was dissolved in anhydrous dichloromethane (50 mL). Et_3N (150 μL, 1.07 mmol) was added to the above solution and stirred for 15 min in an ice bath, and then isophthaloyl chloride (0.079 g, 0.39 mmol) was added. The mixture was slowly warmed up to room temperature and monitored by TLC. After 8 h, the reaction was complete. The solution was rotary evaporated to dryness under the vacuum. The purple solid was obtained and purified by column chromatography (silica, pure CH_2Cl_2) (yield 0.48 g, 74%). ^{1}H NMR (400 MHz, $CDCl_3$): δ 8.82 (8 H, m), 8.67 (4 H, d), 8.56 (4 H, d), 8.31 (2 H, d), 8.14 (8 H, m), 7.93 (6 H, m), 7.77 (16 H, m), 7.55 (4 H, m), 7.45 (2 H, t), 7.27 (2 H, s), 6.62 (1 H, s), 5.52 (2 H, d), 5.23 (2 H, t) −2.89 (4 H, s). Anal. Calcd for $C_{96}H_{64}N_{10}O_2$: C, 82.98; H, 4.64; N, 10.08. Found: C, 82.99; H, 4.64; N, 10.07.

Preparation of Zinc Bisporphyrinate [Zn_2-1]. *Method 1.* Free base bisporphyrin **1** (0.50 g, 0.35 mmol) was dissolved in the mixture of $CHCl_3$ (200 mL) and CH_3OH (100 mL), and $Zn(CH_3COO)_2$ (0.25g 1.4 mmol) was added to the above solution and refluxed. After 2 h, it was extracted with chloroform, and then the organic layer was separated and rotary evaporated to dryness under the vacuum. The purple solid was obtained and purified by column chromatography (silica, CH_2Cl_2/methanol = 99:1) (yield 0.51 g, 95%).

dx.doi.org/10.1021/ic401949e | Inorg. Chem. 2014, 53, 3298−3306

Method 2. The reaction was carried out under anaerobic condition. Zinc 5-(2-aminophenyl)-10,15,20-triphenyl-porphyrinate (0.57 g, 0.79 mmol) was dissolved in anhydrous CH_2Cl_2 (50 mL). Et_3N (150 μL, 1.07 mmol) was added to the above solution and stirred for 15 min in an ice bath, and then isophthaloyl chloride (0.079 g, 0.39 mmol) was added. The mixture was slowly warmed up to room temperature and monitored by TLC. After 8 h, the reaction was complete. The solution was rotary evaporated to dryness under the vacuum. The purple solid was obtained and purified by column chromatography (silica, CH_2Cl_2/methanol = 99:1). Yield 0.48 g, 80%. ^{1}H NMR (400 MHz, $CDCl_3$): δ 8.95 (8 H, m), 8.72 (4 H, d), 8.51 (4 H, d), 8.16 (8 H, m), 7.95 (6 H, m), 7.73 (16 H, m), 7.57 (4 H, m), 7.46 (2 H, t), 7.32 (2 H, d), 7.15 (2 H, s), 5.48 (2 H, d), 5.26 (1 H, t), 4.34 (1 H, s). Anal. Calcd for $C_{96}H_{60}N_{10}O_2Zn_2$ $2H_2O$: C, 74.28; H, 4.16; N, 9.02. Found: C, 74.26; H, 4.13; N, 9.05. [Zn_2-**1**] was dissolved in mixed $CH_2Cl_2/CHCl_3$ (1:1) and transferred into 8 mm × 250 mm glass tubes. Hexane was added as nonsolvent. X-ray quality crystals were obtained after three weeks, see Table 1.

Table 1. Crystal Data and Structural Refinements of [Zn_2-1][11,12]

cryst	[Zn_2-**1**]
chemical formula	$C_{48}H_{29}N_5OZn$
fw	757.13
wavelength (Å)	0.710 73
T	200(2) K
cryst syst	tetragonal
space group	$I4_1$
a (Å)	17.809(2)
b (Å)	17.809(2)
c (Å)	27.080(8)
α (deg)	90
β (deg)	90
γ (deg)	90
V (Å^3)	8589(3)
Z	8
density (g cm^{-3})	1.171
abs coeff (mm^{-1})	0.611
F(000)	3120
data collect θ range	2.31–25.00
index range	$-20 \le h \le 20$
reflns collected	45 143
R_{int}	0.1213
indep reflns	7524
data/restraints/params	7524/76/483
GOF on F^2	1.000
R1[a] [$I > 2\sigma(I)$]	0.0879
wR2	0.2498
residual peak/hole (e/Å^3)	0.496/−0.433
Flack param	0.10(3)

[a] $R1 = \sum(||F_o| - |F_c||)/\sum|F_o|$, $wR2 = \sum w(|F_o|^2 - |F_c|^2)^2/\sum w(|F_o|^2)^2]^{1/2}$.

Preparation of [Zn-2]. Zinc 5-(2-aminophenyl)-10,15,20-triphenylporphyrinate (0.27 g, 0.3 mmol) was dissolved in 30 mL of anhydrous CH_2Cl_2, Et_3N (100 uL, 0.72 mmol) was added to the above solution and stirred for 10 min in an ice bath, and then benzoyl chloride (35 uL, 0.3 mmol) was added dropwise under N_2 condition. The mixture was slowly warmed to room temperature. After 6 h, the reaction was complete. The solution was rotary evaporated to dryness under the vacuum. The purple solid was purified by column chromatography (silica, pure CH_2Cl_2). Yield, 0.144 g, 60%. ^{1}H NMR (400 MHz, $CDCl_3$): δ 8.87 (6 H, m), 8.50 (2 H, m), 8.26 (1 H, s), 8.17 (5 H, m), 8.02 (1 H, m), 7.70 (10 H, d), 7.52 (2 H, m), 7.38 (1 H, s), 7.28 (4 H, m), 6.56 (1 H, m). Anal. Calcd for $C_{51}H_{33}N_5OZn$ H_2O: C, 75.14; H, 4.33; N, 8.59. Found: C, 75.15; H, 4.30; N, 8.57.

X-ray Structure Determination. See details in Table 1.

RESULTS AND DISCUSSION

Crystal Structure and CD Spectra of [Zn_2-1]. Single crystals of [Zn_2-**1**] were obtained by diffusion of hexane into its $CH_2Cl_2/CHCl_3$ solution. The structure of one single crystal was solved in the space group $I4_1$. One asymmetric unit consists of half a bisporphyrin molecule. The whole molecule is shown in Figure 2; the single molecule is just an *m*-phthalic diamide-linked zinc bisporphyrinate as designed. The single molecule does not have mirror symmetry, but has rotational symmetry, which leads to a chiral bisporphyrin as a clockwise twist. The angle between the projections of the electric transition moments $B_{\|}$ and $B_{\|}'$ is 53.8°, which is much different from that of the oxalic amide-linked bisporphyrin (156.0° for the calculated structure).[5e] This indicates that the *m*-phthalic diamide linkage is more flexible, and the corresponding intertransition angle could be much closer to the 70°, the best angle for the coupling.[7,8]

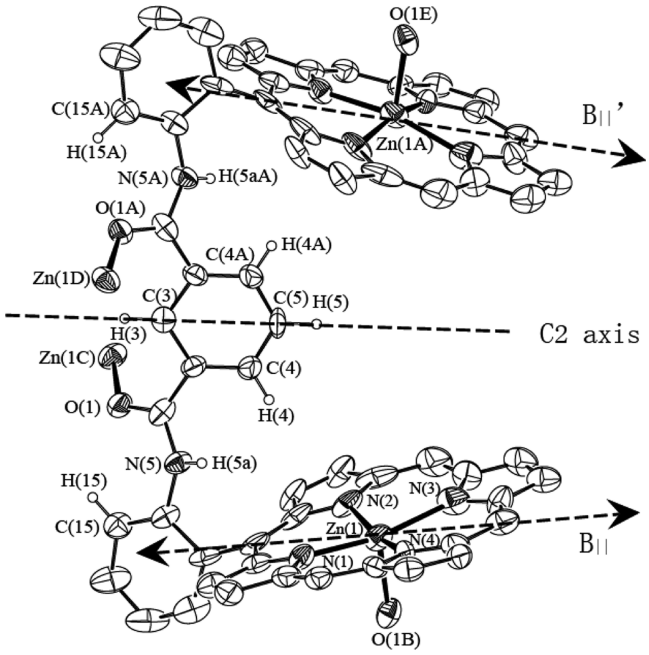

Figure 2. ORTEP diagram of [Zn_2-**1**]. 30% probability ellipsoids are depicted. Zn(1)−O(1B) = 2.201(6) Å, Zn(1)−N(1) = 2.019(7) Å, Zn(1)−N(2) = 2.054(7) Å, Zn(1)−N(3) = 2.083(9) Å, Zn(1)−N(4) = 2.033(7) Å. (Symmetry operator: A, $1-x, 1-y, z$; B, $1-y, {}^1/_2+x, {}^1/_4+z$; C, $-{}^1/_2+y, 1-x, -{}^1/_4+z$; D, ${}^3/_2-y, x, -{}^1/_4+z$; E, $y, {}^1/_2-x, {}^1/_4+z$.) Besides H(3), H(4), H(5), H(15), and H(5a), other hydrogen atoms and six phenyl groups at *meso*-position are omitted for clarity. The C_2 axis and electronic transition moments $B_{\|}$ and $B_{\|}'$ have also been labeled.

As shown in Figure 2, in each zinc bisporphyrinate, zinc is not four-coordinate, but five-coordinate. Besides the four pyrrole nitrogen atoms, the fifth coordinated atom is the amide oxygen from its symmetry-related molecule. As illustated in Figure 3, the half bisporphyrin unit marked by the solid circle (containing one zinc and one carbonyl oxygen) is bonded to the neighoring symmetry-related molecule through coordination bonds, which extends along *c* axis (the 4_1 rotation axis) to form a helical chain with *P* configuration as shown in Figure 4.

dx.doi.org/10.1021/ic401949e | Inorg. Chem. 2014, 53, 3298−3306

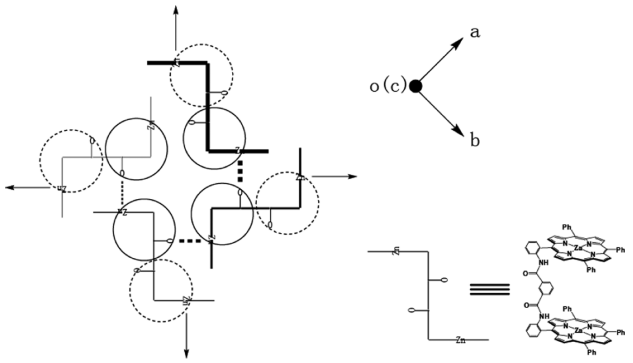

Figure 3. Illustration of the packing structure of [Zn_2-**1**] in the solid state with cell axes labeled. The unit in thicker lines is facing the reader, and the unit in narrower lines is away from the reader.

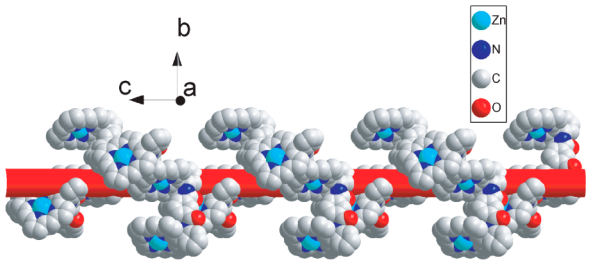

Figure 4. Space-filling representation of the helical chain with *P* configuration of [Zn_2-**1**] formed by Zn−O coordination bonds along *c* axis.

Another half bisporphyrin unit (marked by the dash circle) is also coordinately bonded to the neighboring molecules along the arrow direction to form another helical chain, which extends such a network to three dimension and lead to a chiral coordination polymer. The Flack parameter is 0.10(3), which suggests the handedness of the crystal is correctly assigned.

Such a coordination mode has also caused the phthalic group to be close to the neighboring porphyrin molecule. Correspondingly, it leads to some close interactions. As shown in Figure 5, two of the closest hydrogen to porphyrin plane distances are 2.79 Å for H(15) and 3.04 Å for H(3). More interestingly, such interactions exist not only in solid state, but also in solution, which has been confirmed by UV−vis and ^{1}H NMR spectroscopic studies (vide infra).

To confirm the chirality of the single crystals, CD spectroscopy has been applied on crystalline samples. Single

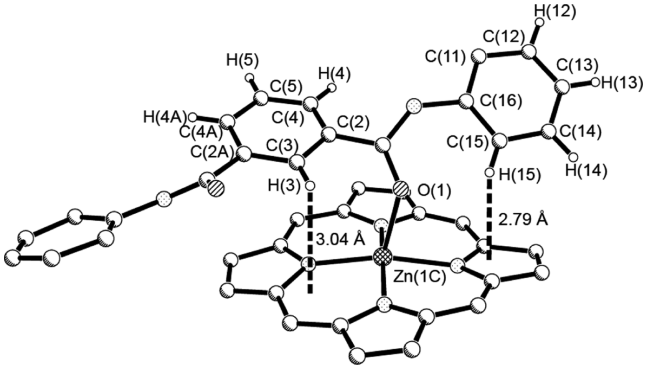

Figure 5. Hydrogen to porphyrin interactions in the crystal structure of [Zn_2-**1**]. (Symmetry operator: C, $-^1/_2 + y$, $1 - x$, $-^1/_4 + z$.)

crystals were randomly picked up. KBr pellets were prepared by grinding each crystal sample with solid potassium bromide (KBr) and applying great pressure to the dry mixture. The measured spectra exhibited remarkable CD absorption in the Soret band region. It confirms the chirality of single crystals. Spectra of two selected single crystals are presented in Figure 6,

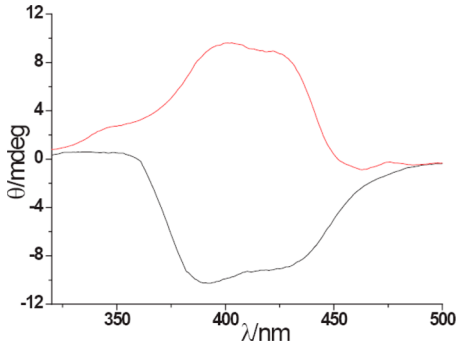

Figure 6. CD spectra of crystallites of [Zn_2-**1**] in KBr pellets. The two pellets were prepared using selected crystals, and showed enantiomeric CD patterns that provide definitive evidence that spontaneous resolution had occurred.

which clearly show broad positive or negative absorptions in the Soret band region. Such enantiomeric CD spectra provide definitive evidence that spontaneous resolution has occurred during the crystallization process.

Aggregation of [Zn_2-1] in Solution. UV−vis spectra of [Zn_2-**1**] have been measured in CH_2Cl_2 and shown in Figure 7.

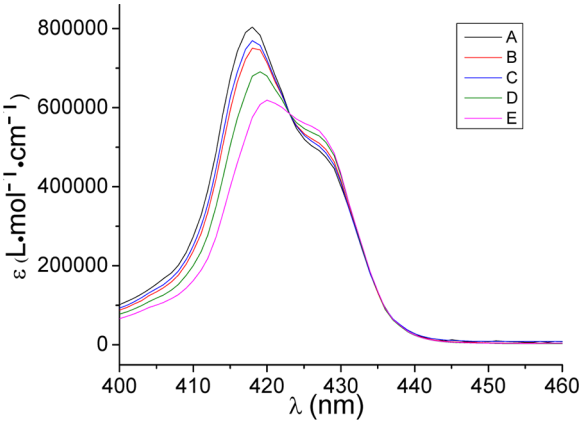

Figure 7. UV−vis spectra of [Zn_2-**1**] in 0.1 mm, 1 mm, and 1.0 cm quartz cell for different concentration as (A) 1.63×10^{-7} M, (B) 8.13×10^{-7} M, (C) 1.63×10^{-6} M, (D) 1.63×10^{-5} M, (E) 1.63×10^{-4} M in methylene dichloride.

Interestingly, the spectra of [Zn_2-**1**] show one strong Soret band at 418 nm and one shoulder at 427 nm, whereas, for the oxalic amide-linked species, there is no such shoulder.[5e] Generally, for bisporphyrin systems, when the two porphyrin moieties are oriented in a parallel manner, the $\pi-\pi$ interactions could lead to hypsochromic shifts of the Soret band in comparison to the porphyrin monomer.[13] On the other hand, the coordination of zinc porphyrin to oxygen or nitrogen in general leads to bathochromic shifts as compared to four-coordinate zinc porphyrins.[14] In our case, such a shoulder at longer wavelengh could be caused by the second reason. For comparison, the metal free bisporphyrin **1** has also been

dx.doi.org/10.1021/ic401949e | *Inorg. Chem.* 2014, 53, 3298−3306

measured by UV−vis spectroscopy. The spectrum is provided in Supporting Information Figure S1, which does not show such a shoulder. This suggests that the zinc is possibly involved in the formation of such a shoulder. One possibility is that that zinc is coordinated with the carbonyl oxygen from neighboring bisporphyrin as shown in the solid structure. Another possibility is that the additional Zn···O═C bond may be intramolecular (for the monomeric form in solution). However, the solid structure shows that the intramolecular Zn···O distances are 7.77 and 9.76 Å, and the linkage is still quite rigid. So this intramolecular interaction is less likely. So the above spectral changes suggest the aggregation through the coordination bonds occurs in solution, and the following equilibrium (eq 1) exists in solution. $[Zn_2\text{-}\mathbf{1}]_n$ is the aggregated species, and $[Zn_2\text{-}\mathbf{1}]$ is the single zinc bisporphyrinate molecule. Since the polymer solubility is usually poor, the dissolved species in solution is most likely the aggregated species with small interger numbers *n*.

$$[Zn_2\text{-}\mathbf{1}]_n \rightleftharpoons [Zn_2\text{-}\mathbf{1}] \quad (1)$$

Such an explanation is supported by UV−vis spectra measured at variable concentrations as shown in Figure 7. This showed that when the concentration of $[Zn_2\text{-}\mathbf{1}]$ increased, the intensity of the shoulder increased, and the intensity of the peak at 418 nm decreased. The corresponding ratio between their molar absorptions increased, which suggests that the ratio between the aggregated species and the single molecule increases with the increasing concentration. This is consistent with the equilibrium (eq 1). For such an equilibrium, when the concentrations increase, the equilibrium in eq 1 shifts to the reverse direction, and the ratio between $[Zn_2\text{-}\mathbf{1}]_n$ and $[Zn_2\text{-}\mathbf{1}]$ increases. As we also notice, when the concentration increases, the bandwidth of the Soret band becomes sharper. The bandwidth change has been reported to be related to the conformational flexibility.[15] In our case, the aggregated species is likely less flexible than the monomeric species, the decreased conformational flexibility would give rise to a narrower distrubution of the excited state vibrational levels, and thus the Soret band became sharper.

NMR also reveals interesting features in solution. For the metal free bisporphyrin **1**, except the NH protons, all other protons are aromatic protons. The resonances for such a kind of protons are generally located in the 7−9 ppm region.[16] Pyrrole protons are usually located at 8.5−9.0 ppm, and phenyl protons are located in the 7−8.5 ppm region. As shown in Figure 8, there are resonances at 6.61, 5.53, and 5.25 ppm. Integration suggests they correspond to 1, 2, 1 protons. Because of the symmetry of the whole molecule, the single proton can only be assigned to the phthalic group. Compared with phenyl protons in 1,3-benzenedicarboxamide,[17] these resonances shift upfield. Since the phthalic group is between two porphyrin subunits, such upfield shifts are most likely due to the ring current effect of porphyrin. The splitting patterns (singlet, doublet, triplet) are consistent with H(3), H(4), and H(5), respectively. Such an assignment is also confirmed by $^1H-^1H$ COSY (see Supporting Information Figure S2). The resonance of H(15) is located at 8.31 ppm. The NH signal is assigned at 7.27 ppm according to the ^1H NMR spectrum recorded upon addition of D_2O (Supporting Information Figure S3).

Compared with the metal free bisporphyrin **1**, most signals for the zinc bisporphyrinate $[Zn_2\text{-}\mathbf{1}]$ remain unchanged, while the resonances of H(3) and H(15) shifted remarkably upfield to 4.38 and 7.34 ppm. The corresponding shifts are 2.24 and

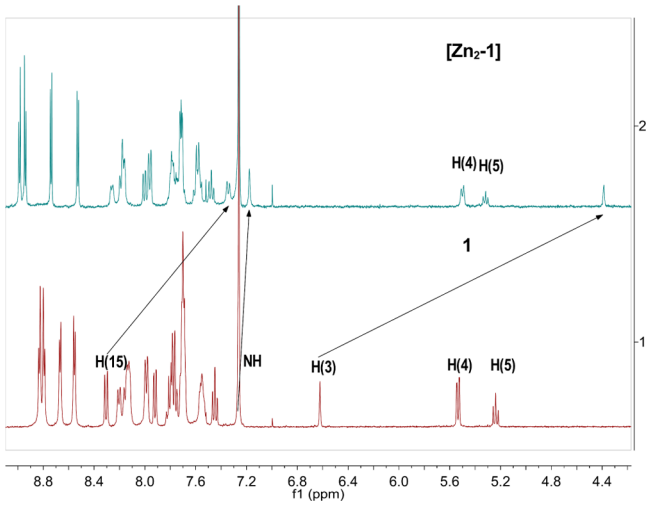

Figure 8. Comparison of the ^1H NMR spectra for $[Zn_2\text{-}\mathbf{1}]$ (1.3×10^{-3} M) and **1** (3.0×10^{-3} M).

0.97 ppm, respectively. Considering their positions in the solid structure, it is likely that the upfield shifts are caused by the aggregation in solution. When the carbonyl oxygen is coordinated to the zinc in a symmetry related porphyrin, it forces these protons over the porphyrin plane; the ring current effect causes such upfield shifts (vide supra). This is also consistent with the UV−vis spectroscopic study.

In addition, ^1H NMR spectra at different temperature or different concentrations have also been measured and presented in Figure 9 and Supporting Information Figure S4.

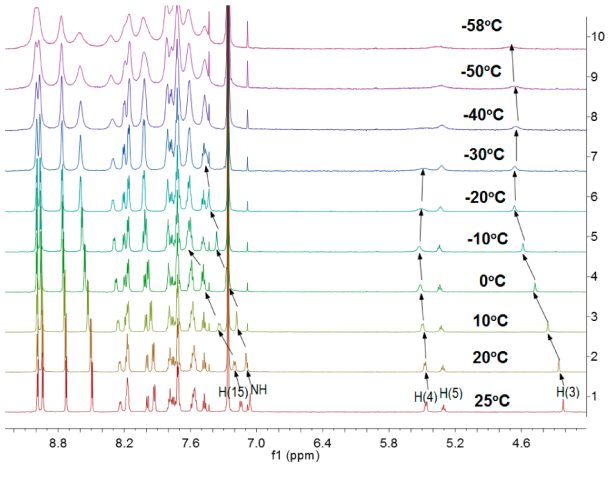

Figure 9. ^1H NMR for $[Zn_2\text{-}\mathbf{1}]$ (1.3×10^{-3} M) at variable temperature.

In these spectra, most resonances do not change; only the resonances of H(3), H(15), and NH have shown slight shifts. When the temeprature was down to −30 °C or below, the signals of H(15) and NH were overlapped with aromatic protons, and became indistinguishable. These spectral changes suggest that the overall conformation of bisporphyrin does not change in this process or changes very little, but the chemical environments of H(3), H(15) and NH do change. It is likely due to the equilibrium in eq 1 in solution.

As shown in Figure 9, when the temperature decreased, all the ^1H NMR signals became broader. Several factors could cause such line broadening. (i) As suggested by eq 1, there are

dx.doi.org/10.1021/ic401949e | Inorg. Chem. 2014, 53, 3298−3306

both $[Zn_2\text{-}\mathbf{1}]_n$ and $[Zn_2\text{-}\mathbf{1}]$ in the solution. (ii) There could be multiple conformers in solution. The observed signals are contributed by all these species. At low temperature, the relatively slow exchanges between these species could cause line broadening. For such cases, if temperature is low enough, we could observe splitting of the signals. Unfortunately, no splitting was observed when the temperature was down to −58 °C, the lowest temperature we can reach. (iii) Another factor could be due to the quadrupole relaxation of ^{14}N nucleus. The quadrupole relaxation of ^{14}N nucleus can have effects on the nearby magnetic nuclei since rapid quadrupole relaxation can broaden *J*-coupling between the two nuclei and lead to line broadening. It has been reported that the quadrupole relaxation of ^{14}N became faster at lower temperature for the ammonium ions, therefore leading to the line broadening.[18] Such broadening is related to the distance between the two nuclei. In our case, the signals of H(4) became much broader than H(3) and H(5) at lower temperature, which is consistent with the fact that the N···H(4) (2.70 Å) is much shorter than N···H(3) (3.80 Å) and N···H(5) (4.84 Å) in the solid structure.

Chiral Recognition of Amino Acid Esters. Besides the spontanous resolution of crystals of $[Zn_2\text{-}\mathbf{1}]$ and its aggregation behavior in solution, we are very interested in its chiral recognition ability for chiral guests, such as amino acid esters. So five pairs of amino acid esters shown in Figure 1 have been tested. $[Zn_2\text{-}\mathbf{1}]$ and enantiopure D- or L-amino acid ethyl esters were mixed in methylene dichloride, and the corresponding CD spectra were measured. For all these amino acid esters, the spectra showed bisignate Cotton effects with strong intensities in the Soret band region. One example for phenylglycine ethyl ester is displayed in Figure 10, and others are shown in Figures

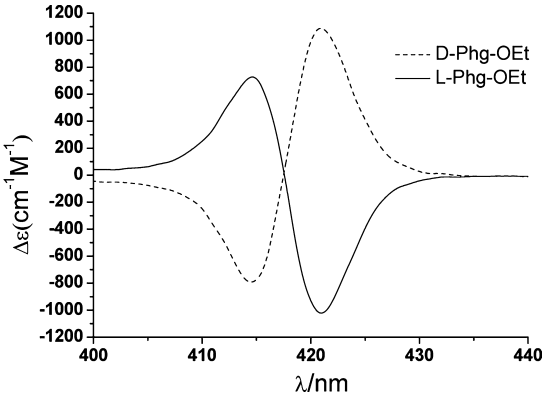

Figure 10. Circular dichroism spectra of a solution of $[Zn_2\text{-}\mathbf{1}]$ (2.40×10^{-6} M) and 4000 equiv of L- (solid line) and D- (dash line) phenylglycine ethyl ester in methylene dichloride at 25 °C.

S5−S8 in Supporting Information. Their titration spectra are also provided in Supporting Information Figures S9−S13. For all L-type guests, the corresponding longer-wavelength peak of the Soret band was negative, and the shorter-wavelength peak was positive. On the other hand, the spectra of the complexes formed between $[Zn_2\text{-}\mathbf{1}]$ and D-type guests showed similar shape and intensity but with the opposite sign. As listed in Table 2, their amplitude values of CD are about 10 times larger than those for the oxalic amide-linked species[5e] and the ethane-bridged species.[4a] For Phg-OEt, even when the concentration is as low as 8×10^{-6} mol/L, the A_{obs} is around 130 cm^{-1} M^{-1}. Such results suggest that the designed bisporphyrin is a good CD probe to determine the chirality of amino acid esters.

Table 2. Observed CD Spectral Data of the Complexes of $[Zn_2\text{-}\mathbf{1}]$ with Amino Acid Esters in Methylene Dichloride at 25 °C

	λ_{max} (nm) [$\Delta\varepsilon$ (cm^{-1} M^{-1})]		
	1st cotton	2nd cotton	A_{obs} [a]
L-Ala-OEt	421 (−495)	414 (+362)	−857
D-Ala-OEt	421 (+548)	414 (−384)	+932
L-Leu-OEt	421 (−841)	414 (+598)	−1439
D-Leu-OEt	421 (+786)	414 (−578)	+1364
L-Val-OEt	421 (−881)	414 (+665)	−1546
D-Val-OEt	421 (+915)	414 (−703)	+1618
L-Phe-OEt	421 (−959)	414 (+664)	−1623
D-Phe-OEt	421 (+956)	414 (−658)	+1614
L-Phg-OEt	421 (−1057)	414 (+731)	−1788
D-Phg-OEt	421 (+1130)	414 (−797)	+1927

[a] $A_{obs} = \Delta\varepsilon_1 - \Delta\varepsilon_2$. This value represents the total amplitude of the experimentally observed CD couplets.

Besides the much different intensities, their signs are also different from those for the oxalic amide-linked species for the guest with the same handedness, which suggest a possible different chiral recognition mechanism. In order to investigate the interactions between zinc bisporphyrin host and the guest molecules in the chiral recognition process, we have done further studies with ^1H NMR and UV−vis spectroscopies.

^1H NMR Studies. ^1H NMR titration experiments have been performed between $[Zn_2\text{-}\mathbf{1}]$ and D-leucine ethyl ester. The assignments of the signals of the leucine ethyl ester are based on the spectrum measured upon addition of D_2O (Supporting Information Figure S14), the titration spectra (Supporting Information Figure S15) and ^1H−^1H COSY (Supporting Information Figure S18). Upon addition of D_2O, the signal at −3.13 ppm at 25 °C disappeared, which suggests such a signal belongs to NH_2. The titration spectra clearly show the origin of H_d, H_e, H_f, H_g. But the signals of H_a, H_b, and H_c became very broad during the titration, and cannot be tracked in the high concentration of D-Leu-OEt. So we also measured the ^1H−^1H COSY spectrum for the mixture of $[Zn_2\text{-}\mathbf{1}]$ and D-Leu-OEt at −58 °C. However, the 2D spectrum is very difficult to obtain since the solubility of $[Zn_2\text{-}\mathbf{1}]$ is quite low. Supporting Information Figure S18 roughly showed the correlation H_a, H_b, and H_c, which help the assignments. As shown in Figure 11, upon addition of the amino acid ester, the resonances of the ligand protons show remarkable upfield shifts, and indicate the coordination of the ligand (amino acid ester) to the zinc. The shielding effect of the porphyrin ring causes such shifts. Among these CHs, the proton of α carbon has the largest upfield shift, which suggests it is much closer to the porphyrin plane due to the coordination of the ligand to the zinc. Another feature is that the resonances of the methyl protons (H_d and H_e) split into two inequivalent signals in the complex, which indicates the two methyl group have different chemical environment due to the chiral arrangement of the complex.

^1H NMR spectra at variable temperature have also been measured for this sample. Figure 11 shows that all the signals become broader at −30 °C. When temperature reached −58 °C, the splittings for NH_2, H_a, H_b, H_c, H_d, and H_f of the guest molecule were observed. Among them, the splitting of NH_2 is especially interesting. The signals of NH_2 change from one singlet at room temperature to two doublets at −58 °C. Each doublet is contributed from one NH_2 proton, which suggests these two NH_2 protons are chemically inequivalent. The

dx.doi.org/10.1021/ic401949e | Inorg. Chem. 2014, 53, 3298−3306

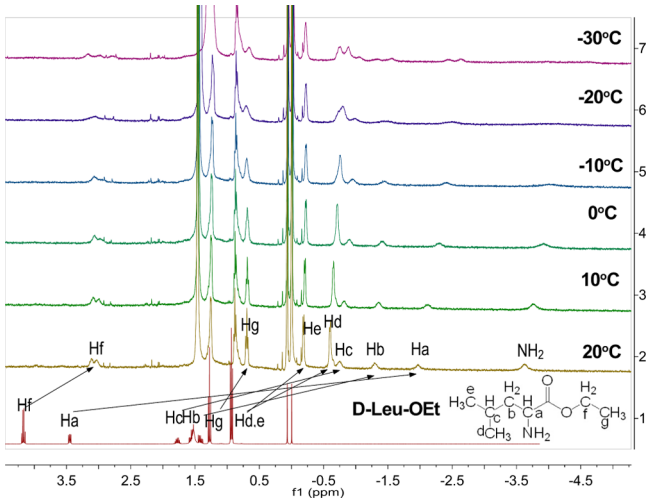

Figure 11. ^{1}H NMR of D-leucine ethyl ester (bottom), and the mixture of [Zn_2-**1**] (0.5×10^{-3} M) and D-leucine ethyl ester (0.7 equiv, top 10) at different temperatures.

splitting of NH_2 resonance into two signals can be explained by the following: when the leucine ethyl ester is coordinated to the zinc porphyrinate, two NH_2 protons become chemically inequivalent due to the overall chiral arrangements of the host–guest complex. There is the exchange between the coordinated ligands and uncoordinated ligands in solution. At high temperature, such exchange is too fast. At low temperature, this exchange becomes slow, which allows NMR to record the signals of each NH_2 proton separately. The further splitting of each NH_2 proton could be due to the following reasons: (i) there are a 1:1 complex and a 1:2 complex in the solution, and the coordinated leucine ethyl esters in each species are different; (ii) even for the 1:2 complex, two leucine ethyl esters are chemically inequivalent because of the chiral arrangements of the overall complex; (iii) there are multiple conformers of the leucine ethyl ester in solution. Currently, we do not have enough evidence to distinguish which is the dominant factor. They could all contribute to the observed NMR spectra.

We have done several titration experiements, and presented three of them in Supporting Information Figures S15–S17. Each titration used different amounts of D-leucine ethyl ester in order to show clearly the changes in different regions. In the Supporting Information, Figure S15 shows the −4.0 to 4.0 ppm region, Figure S16 shows the 4.0 to 6.6 ppm region, and Figure S17 shows the 7.0 to 9.0 ppm region. These spectra showed the resonances of H(3), H(15), and NH had significant downfield shifts and further confirmed that the equilibrium (eq 1) is involved in solution. When amino acid ester was added, it will coordinate to [Zn_2-**1**], and make the equilibrium shift in the forward direction, and then the resonance of H(3) shifts downfield. At 6.5 equiv of leucine ethyl ester, the corresponding shifts are 1.51, 0.76, and 0.70 ppm, respectively. Compared with the downfield shift values for the metal free bisporphyrin (Table 3), the shift value for NH is much larger. It indicates there are other contributions. A similar downfield shift for NH was reported by Kuroda et al.,[19] in which there is a contribution from the hydrogen bonds. In our case, such contribution could be due to hydrogen bonds formed between the NH of the amide group and the carbonyl oxygen of guests. We also did CD experiments in which the α-amino alcohol (leucinol) was

Table 3. Lists of Chemical Shifts of H(3), H(15), and NH for [Zn_2-1], 1, and the Mixture of [Zn_2-1] and Leu-OEt

	Chemical shift (ppm)		
	[Zn_2-**1**]	**1**	[Zn_2-**1**] + Leu-OEt (6.5 equiv)
H(3)	4.38	6.62	5.89
H(15)	7.34	8.31	8.10
NH	7.17	7.27	7.87

used as a guest molecule. When such a guest was used, a very weak signal was obtained (Supporting Information Figure S20). This also confirms that the carbonyl oxygen is involved in the above-mentioned hydrogen bonds in the chiral recognition process. So, ^{1}H NMR spectra suggest there are coordination interactions and hydrogen bonding interactions between host and guest molecules.

UV–Vis Spectra. UV–vis spectroscopic titrations have been performed between the zinc bisporphyrinate and five amino acid ethyl esters. A representative example of the spectral change of [Zn_2-**1**] induced by the addition of L-Phe-OEt is shown in Figure 12. (Others are provided in Supporting

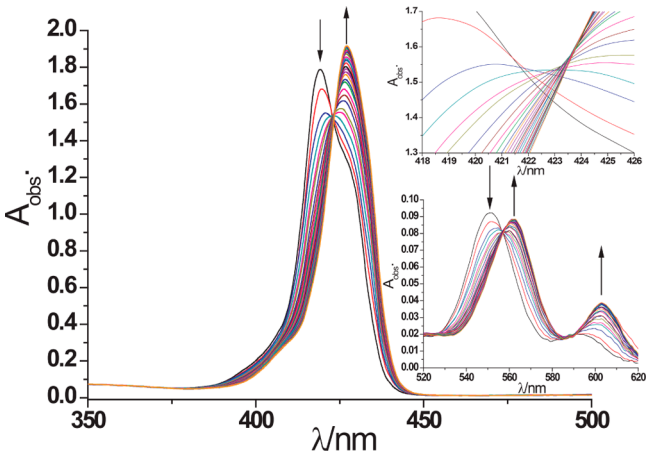

Figure 12. UV–vis spectral changes of [Zn_2-**1**] (2.40×10^{-6} M) in methylene dichloride upon addition of L-Phg-OEt. The host to guest molar ratio changes from 1:0 to 1:200 at 25 °C. Arrows indicate absorbance changes with increasing guest concentrations.

Information Figures S21–S26). Before the addition, the spectrum of [Zn_2-**1**] shows one strong Soret band at 418 nm and one shoulder at 427 nm. During the titration, the electronic spectra showed that the intensity of band at 418 nm decreased and the intensity at 427 nm increased by the increasing of the ligand concentrations.

In solution, the ^{1}H NMR spectra suggest that the amino acid ester in the complex presents a hydrogen bond between the carbonyl oxygen and the amide NH, and it also indicates that all amino acid esters function as monodentate ligands since there is only one binding site left except carbonyl oxygen. This is also similar to the case of the oxalic amide-linked species in which it has been observed a monodentate behavior of the amino acid ester in the crystal structure.[5e] In other cases, when a bidentate ligand is used, remarkable CD spectral changes have been observed at high ligand molar excess.[20,3b] Such spectral changes were not observed in this study (see Supporting Information Figures S9–S13). So all these suggest amino acid esters function as mondentate ligands.

dx.doi.org/10.1021/ic401949e | Inorg. Chem. 2014, 53, 3298–3306

As shown in Figure 12, there are at least two pseudoisosbestic points upon titration, which are very close to each other. Compared with the oxalic amide-linked species,[5e] the above UV−vis spectroscopic changes could be interpreted as being due to the formation of 1:2 complexes between the [Zn_2-**1**] and the amino acid esters, where such complexation requires two steps. The first step is the formation of a 1:l complex (eq 2), and the second step is the formation of a 1:2 complex (eq 3). However, because three equilibria are shown in solution, the corresponding binding constants K_1 and K_2 are difficult to obtain.

$$[Zn_2\text{-}\mathbf{1}] + L \overset{K_1}{\rightleftharpoons} [Zn_2\text{-}\mathbf{1}]\cdot L \quad (2)$$

$$[Zn_2\text{-}\mathbf{1}]\cdot L + L \overset{K_2}{\rightleftharpoons} [Zn_2\text{-}\mathbf{1}]\cdot (L)_2 \quad (3)$$

Since this system is similar to the oxalic amide-linked case, the titration spectra are also similar; it is reasonable to consider that K_1 and K_2 have similar values as that case. For the oxalic amide-linked species, the K_1 is much larger than K_2. When the amino acid ester is in low concentration (such as 1×10^{-5} M), the [Zn_2-**1**]·L species is the dominant species, while the intensity of the CD at such a concentration is still strong. When the concentration is much higher, [Zn_2-**1**]·$(L)_2$ becomes the dominant species, and the intensity of the CD increases to the maximum value. This suggests both [Zn_2-**1**]·L and [Zn_2-**1**]·$(L)_2$ species have contributions to the CD signals.

Chiral Recognition Mechanism. The above studies suggest coordination interactions and hydrogen bonding interactions make the ligand bind tightly on zinc porphyrinate. Such a binding mode is similar to the monomeric zinc porphyrinate system bearing two naphthol groups reported by Ogoshi and Mizutani.[21] Their proposed mechanism suggested that the induced CD was caused by the coupling between the magnetic transition dipole moment of the carbonyl group of the guest molecule and the electric transition dipole moment of the Soret band of the porphyrin host. In the system presented in this Article, the amplitudes of induced CD are around 40 times stronger than theirs. Thus, their mechanism is not appropriate for our system. Extra evidence has been further provided by a comparison experiment with [Zn-**2**] as the host. When such a monoporphyrin species was mixed with enantiopure amino acid ethyl ester, no observable signal was obtained. So the induced CD is most likely contributed from the chromophore interactions within the bisporphyrin host.

In such a binding mode, because of the position of the amide group, hydrogen bonds make the ligand coordinate to zinc in the intraporphyrin core side. So it is possible to cause the steric interactions between host and guest molecules. Such a steric effect is actually evidenced by the fact that the CD amplitude values are dependent on the bulkiness of the side chain (R) of amino acid ester series. As shown in Table 2, the CD amplitude values are in the following order: Phg-OEt > Phe-OEt ~ Val-OEt > Leu-OEt > Ala-OEt. If we consider the structures of these amino acid esters as shown in Figure 1, such an order is consistent with the bulkiness of substituents on the β carbons. This also suggest that the β carbon is in close contact with the other porphyrin subunit when the amino acid ester is coordinated to one zinc porphyrinate.

On the basis of the above, we propose a possible chiral recognition mechanism as shown in Figure 13. When the amino acid ester is mixed with [Zn_2-**1**], it functions as a monodentate ligand to form 1:1 complex (major species at low concentration) and 1:2 complex (major species at higher concentration). For clarity, only the case for 1:1 complex is shown. The guest molecules interact with the zinc bisporphyrinates by coordination interactions, hydrogen bonds, and steric interactions. When the D-amino acid ester is used, two possible complexes may form, having a quasienantiomeric interporphyrinic arrangement. In the most stable arrangement, the hydrogen is clamped between the two porphyrins, while the R group (side chain group) with a larger size than hydrogen tends to point away from the intraporphyrin core. In this preferred conformation, the two porphyrins adopt a clockwise twist. Then, in the solution such a conformer will be the dominant species thus leading to the positive CD couplet in the Soret band region. Increasing the substituent's bulkiness results in an increase of the degree of right-handed screw as a result of the above-mentioned steric interactions. According to the CD exciton chirality theory,[6] the spatial orientation of the optically active electronic transitions in the more screw structure of bisporphyrinates produces an induced CD signal of higher intensity, and vice versa. For the 1:2 complex, the insertion of second ligand into the intraporphyrin cavity could increase the degree of right-handed screw, and so increase the intensity of the CD signal. For the L-type guest, the resulting bisporphyrinate with different screw sense gives opposite signs of their corresponding Cotton effects. These are consistent with the experimental results.

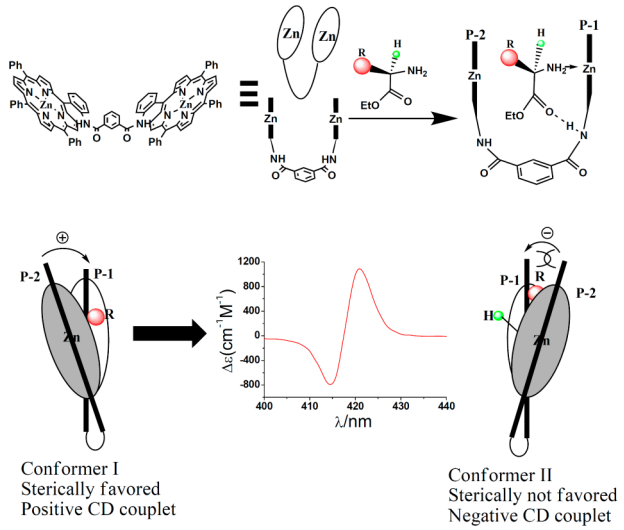

Figure 13. Proposed chiral recognition mechanism. Complexation of [Zn_2-**1**] with D-amino acid ester can adopt two conformations: (I) with the R group projecting out of the intraporphyrin core and (II) with the H group projecting out of the intraporphyrin core. The positive sign of the couplet is in agreement with the energetically favored conformer I. For clarity, only the case for 1:1 complex is shown.

CONCLUSION

We have designed and synthesized an *m*-phthalic diamide linked zinc bisporphyrinate. Its chiral crystalline samples have been obtained by spontaneous resolution. The structure reveals each zinc atom is coordinated to the amide oxygen of the neighboring molecule. It forms a helical chain along the *c* axis, and the overall crystal forms a chiral coordination polymer. Such a zinc bisporphyrinate has shown remarkable chiral recognition ability for amino acid esters. Our studies suggest this new bisporphyrinate is a good chiral recognition host for

dx.doi.org/10.1021/ic401949e | Inorg. Chem. 2014, 53, 3298−3306

monodentate ligands. Further investigations on other monodentate chiral molecules are ongoing.

■ ASSOCIATED CONTENT

Supporting Information

CD spectra of a solution of [Zn_2-**1**] with four amino acid esters, CD titration spectra, NMR spectra, CD spectra of a solution of [Zn_2-**1**] with D/L-leucinol, UV−vis spectra upon titration, and crystallographic data (CCDC949004) in CIF format. This material is available free of charge via the Internet at http://pubs.acs.org.

■ AUTHOR INFORMATION

Corresponding Author

*E-mail: cjhu@suda.edu.cn.

Author Contributions

‖J.J. and X.F. contributed equally.

Notes

The authors declare no competing financial interest.

■ ACKNOWLEDGMENTS

We thank the National Nature Science Foundation of China for financial support (Nos. 20971093 and 21271133) and the Priority Academic Program Development of Jiangsu Higher Education Institutions. We also thank W. R. Scheidt (University of Notre Dame) for help with the manuscript preparation.

■ REFERENCES

(1) (a) Hembury, G. A.; Borovkov, V. V.; Inoue, Y. *Chem. Rev.* **2008**, *108*, 1. (b) Berova, N.; Pescitelli, G.; Petrovica, A. G.; Pronic, G. *Chem. Commun.* **2009**, 5958. (c) Rosaria, L.; Durso, A.; Mammana, A.; Purrello, R. *Chirality* **2008**, *20*, 411.

(2) (a) Huang, X.; Rickman, B. H.; Borhan, B.; Berova, N.; Nakanishi, K. *J. Am. Chem. Soc.* **1998**, *120*, 6185. (b) Kurtàn, T.; Nesnas, N.; Koehn, F. E.; Li, Y.; Nakanishi, K.; Berova, N. *J. Am. Chem. Soc.* **2001**, *123*, 5974. (c) Huang, X. F.; Borhan, B.; Rickman, B. H.; Nakanishi, K.; Berova, N. *Chem.—Eur. J.* **2000**, *6*, 216. (d) Huang, X.; Fujioka, N.; Pescitelli, G.; Koehn, F. E.; Williamson, R. T.; Nakanishi, K.; Berova, N. *J. Am. Chem. Soc.* **2002**, *124*, 10320. (e) Kurtan, T.; Nesnas, N.; Li, Y. Q.; Huang, X. F.; Nakanishi, K.; Berova, N. *J. Am. Chem. Soc.* **2001**, *123*, 5962. (f) Proni, G.; Pescitelli, G.; Huang, X. F.; Quraishi, N. Q.; Nakanishi, K.; Berova, N. *Chem. Commun.* **2002**, 1590.

(3) (a) Li, X.; Borhan, B. *J. Am. Chem. Soc.* **2008**, *130*, 16126. (b) Li, X.; Tanasova, M.; Vasileiou, C.; Borhan, B. *J. Am. Chem. Soc.* **2008**, *130*, 1885.

(4) (a) Borovkov, V. V.; Yamamoto, N.; Lintuluoto, J. M.; Tanaka, T.; Inoue, Y. *Chirality* **2001**, *13*, 329. (b) Borovkov, V. V.; Hembury, G. A.; Yamamoto, N.; Inoue, Y. *J. Phys. Chem. A* **2003**, *107*, 8677. (c) Borovkov, V. V.; Hembury, G. A.; Inoue, Y. *Acc. Chem. Res.* **2004**, *37*, 449.

(5) (a) Hu, C.; Noll, B. C.; Piccoli, P. M. B.; Schultz, A. J.; Schulz, C. E.; Scheidt, W. R. *J. Am. Chem. Soc.* **2008**, *130*, 3127. (b) Hu, C.; Sulok, C. D.; Paulat, F.; Lehnert, N.; Twigg, A. I.; Hendrich, M. P.; Schulz, C. E.; Scheidt, W. R. *J. Am. Chem. Soc.* **2010**, *132*, 3737. (c) Yang, J.; Jiang, J.; Fang, W.; Kai, X.; Hu, C.; Yang, Y. *J. Porphryins Phthalocyanines* **2011**, *15*, 197. (d) Kai, X.; Jiang, J.; Hu, C. *Chem. Commun.* **2012**, 4302. (e) Jiang, J.; Feng, Z.; Liu, B.; Hu, C.; Wang, Y. *Dalton Trans.* **2013**, *42*, 7651.

(6) Berova, N.; Nakanishi, K.; Woody, R. W. *Circular Dichroism: Principles and Applications*, 2nd ed.; Wiley-VCH: New York, 2000.

(7) Harada, N.; Nakanishi, K. *Circular Dichroism Spectroscopy—Exciton Coupling in Organic Stereochemistry*; University Science Books: Mill Valley, CA, 1983.

(8) Yoshida, N.; Ishizuka, T.; Osuka, A.; Jeong, D. H.; Cho, H. S.; Kim, D.; Matsuzaki, Y.; Nogami, A.; Tanaka, K. *Chem.—Eur. J.* **2003**, *9*, 58.

(9) Otto, K. E.; Hesse, S.; Wassermann, T. N.; Rice, C. A.; Suhm, M. A.; Stafforst, T.; Diedesen, U. *Phys. Chem. Chem. Phys.* **2011**, *13*, 14119.

(10) Goudriaan, P. E.; Jang, X.-B.; Kuil, M. *Eur. J. Org. Chem.* **2008**, *36*, 6079.

(11) Sheldrick, G. M. *Acta Crystallogr., Sect. A* **2008**, *64*, 112.

(12) Spek, A. L. *J. Appl. Crystallogr.* **2003**, *36*, 7.

(13) (a) Hunter, C. A.; Meah, M. N.; Sanders, J. K. M. *J. Am. Chem. Soc.* **1990**, *112*, 5773. (b) Hunter, C. A.; Leighton, P.; Sanders, J. K. M. *J. Chem. Soc., Perkin Trans.* **1989**, *1*, 547. (c) Gouterman, M.; Holten, D.; Lieberman, E. *Chem. Phys.* **1977**, *25*, 139. (d) Hunter, C. A.; Sanders, J. K. M.; Stone, A. *J. Chem. Phys.* **1989**, *133*, 395. (e) Crossley, M. J.; Hambley, T. W.; Mackay, L. G.; Try, A. C.; Walton, R. *J. Chem. Soc., Chem. Commun.* **1995**, 1077.

(14) Nardo, J. V.; Dawson, J. H. *Inorg. Chim. Acta* **1986**, *123*, 9.

(15) Huang, X.; Borhan, B. H.; Berova, N.; Nakanishi, K. *J. Indian Chem. Soc.* **1998**, *75*, 725.

(16) Medforth, C. J. In *The Porphyrin Handbook*; Kadish, K., Smith, K., Guilard, R., Eds.; Academic Press: New York, 2000; Vol. 5, Chapter 35.

(17) Marlin, D. S.; Olmstead, M. M.; Mascharak, P. K. *J. Mol. Struct.* **2000**, *554*, 211.

(18) (a) Richard, A. O., Jr.; James, D. R. *J. Chem. Phys.* **1957**, *26*, 1340. (b) Halliday, J. D.; Bindner, P. E.; Pasamshi, S. *Can. J. Chem.* **1985**, *63*, 2975.

(19) Kuroda, Y.; Kato, Y.; Higashioji, T.; Hasegawa, J.; Kawanami, S.; Takahashi, M.; Shiraishi, N.; Tanabe, K.; Ogoshi, H. *J. Am. Chem. Soc.* **1995**, *117*, 10950.

(20) Borovkov, V. V.; Lintuluoto, J. M.; Hembury, G. A.; Sugiura, M.; Arakawa, R.; Inoue, Y. *J. Org. Chem.* **2003**, *68*, 7176−7192.

(21) Mizutani, T.; Ema, T.; Yoshida, Y.; Kuroda, Y.; Ogoshi, H. *Inorg. Chem.* **1993**, *32*, 2072.